JPEDAV (2006) 27:665-670
DOI: 10.1361/154770306X153710
1547-7037/$19.00 ©ASM International

Interdiffusion in γ (Face-Centered Cubic) Ni-Cr-*X* (*X* = Al, Si, Ge, or Pd) Alloys at 900 °C

Narayana Garimella, and M.P. Brady, and Yongho Sohn

(Submitted April 3, 2006; in revised form July 19, 2006)

Interdiffusion in nickel (Ni)-chromium (Cr) (face-centered cubic γ phase) alloys with small additions of aluminum (Al), silicon (Si), germanium (Ge), or palladium (Pd) was investigated using solid-to-solid diffusion couples. Ni-Cr-*X* alloys having compositions of Ni-22at.%Cr, Ni-21at.%Cr-6.2at.%Al, Ni-22at.%Cr-4.0at.%Si, Ni-22at.%Cr-1.6at.%Ge, and Ni-22at.%Cr-1.6at.%Pd were manufactured by arc casting. The diffusion couples were assembled in an Invar steel jig, encapsulated in Ar after several hydrogen purges, and annealed at 900 °C in a three-zone tube furnace for 168 h. Experimental concentration profiles were determined from polished cross sections of these couples by using electron probe microanalysis with pure element standards. Interdiffusion fluxes of individual components were calculated directly from the experimental concentration profiles, and the moments of interdiffusion fluxes were examined to determine the average ternary interdiffusion coefficients. The effects of ternary alloying additions on the diffusional behavior of Ni-Cr-X alloys are presented in the light of the diffusional interactions and the formation of a protective Cr_2O_3 scale.

Keywords Boltzmann/Matano analysis, diffusion couples, diffusivity coefficient, experimental study, interdiffusion, multicomponent diffusion, ternary system

1. Introduction

Nickel (Ni)-chromium (Cr)-base alloys are widely used in a variety of high-temperature applications due to their combination of good oxidation resistance and excellent high-temperature strength, and are the basis for a number of commercial superalloy families.[1-3] Oxidation resistance in these alloys is derived from a continuous, slow-growing, adherent C_2O_3-base oxide scale.[1,3] In particular, composition in the range of Ni alloyed with 20-30 wt.% Cr have been extensively studied as a model material for Cr_2O_3 scale formation.[4-13]

Minor alloying additions (<5 wt.%) can significantly improve the oxidation resistance of Ni-base Cr_2O_3-forming alloys.[14-16] Effects include: the establishment of continuous Cr_2O_3 scale formation at reduced Cr concentrations; a decrease in the growth rate of Cr_2O_3; and enhanced scale adherence.[1,14,16] For example, the addition of silicon (Si) in Ni-28wt.%Cr promoted the formation of both Cr_2O_3 and SiO_2,[e.g., 13] in which a continuous inner SiO_2 layer acted as a diffusion barrier, and reduced the isothermal oxidation rate by suppressing cation transport through the Cr_2O_3 scale.[6,13,17-20] However, the same inner SiO_2 layer can also reduce the spallation resistance, which is dependent on the level of Si and on the continuity and thickness of the inner SiO_2 layer formed.[e.g., 21]

Diffusional effects of minor alloy additions may play a significant role in the initial establishment of a continuous protective oxide scale.[2,14,16,22,23] It can also play a significant role in maintaining protective scale growth. For example, the growth of Cr_2O_3 can locally deplete Cr from the alloy in the subsurface region.[e.g., 24] If the scale is locally damaged or spalled, such depletion can prevent the reformation of the Cr_2O_3 scale and result in a transition to less protective or nonprotective oxidation behavior. An understanding of diffusional interactions in Ni-Cr-*X* alloys, where *X* represents minor alloying additions, can help to design Ni-base Cr_2O_3-forming alloys with improved resistance against environmental degradation.[25]

In this work, interdiffusion in Ni-22at.%Cr-*X* [face-centered cubic (fcc) γ phase] alloys with small additions of *X* [*X* = aluminum (Al), Si, germanium (Ge), or palladium (Pd)] is investigated using solid-to-solid diffusion couples at 900 °C for 168 h. This information will be used as a part of a larger study, the goal of which is to better elucidate the effects of minor alloying additions on the oxidation of Cr_2O_3-forming alloys. Additions of Si were selected because it has long been known to be beneficial to Cr_2O_3 scale formation[e.g., 17] via both the establishment of an inner layer of SiO_2 and the possibility of the enhanced diffusivity of Cr. To help probe these effects, additions of Ge were also selected. Ge is thermochemically similar to Si in many regards

This article was presented at the Multicomponent-Multiphase Diffusion Symposium in Honor of Mysore A. Dayananda, which was held during TMS 2006, the 135th Annual Meeting and Exhibition, March 12–16, 2006, in San Antonio, TX. The symposium was organized by Yongho Sohn of University of Central Florida, Carelyn E. Campbell of National Institute of Standards and Technology, Richard D. Sisson, Jr., of Worcester Polytechnic Institute, and John E. Morral of Ohio State University.

Narayana Garimella and **Yongho Sohn,** Advanced Materials Processing and Analysis Center and Department of Mechanical, Materials and Aerospace Engineering, University of Central Florida, Orlando, FL; and **M.P. Brady,** Materials Science and Technology Division, Oak Ridge National Laboratory, Oak Ridge, TN. Contact e-mail: ysohn@mail.ucf.edu.

but does not form a protective oxide scale as does Si. Additions of Al at levels > 3-4 wt.% can improve the oxidation via the formation of a protective Al_2O_3 scale.[2,4,14,16] At subcritical levels (2-3 wt.%), Al may also be beneficial to the oxidation resistance of Ni-Cr alloys, in part via the formation of semicontinuous inner region of Al_2O_3 particles.[26,27] Pd was chosen for the study because it is a noble alloying addition and would be expected to accumulate at the alloy-scale interface during oxidation.[e.g., 28,29]

In this ternary interdiffusion study at 900 °C, the experimental concentration profiles were used to calculate interdiffusion fluxes of individual components, and to determine the average effective interdiffusion coefficients $\tilde{D}_i^{\text{eff}}$ and the average ternary interdiffusion coefficients $\bar{\tilde{D}}_{ij}^{\text{Ni}}$ (i,j = Cr,X). Values of $\tilde{D}_{\text{Cr}}^{\text{eff}}$ and $\bar{\tilde{D}}_{\text{CrX}}^{\text{Ni}}$ are examined to assess the effects of alloying additions on the interdiffusion behavior of Cr, and the Cr_2O_3-forming ability in Ni-Cr-X alloys.

2. Determination of Interdiffusion Coefficients From Ternary Isothermal Diffusion Couples

Onsager's[30] formalism for the interdiffusion flux $\tilde{J}_i$ of component i in a ternary system can be written as:

$$\tilde{J}_i = -\tilde{D}_{i1}^3 \frac{\partial C_1}{\partial \text{x}} - \tilde{D}_{i2}^3 \frac{\partial C_2}{\partial \text{x}} \quad (i, j = 1, 2) \qquad \text{(Eq 1)}$$

where $\partial C_1/\partial x$ and $\partial C_2/\partial x$ are the two independent concentration gradients, and $\tilde{D}_{i1}^3$ and $\tilde{D}_{i2}^3$ refer to the ternary interdiffusion coefficients. An experimental determination of the four concentration-dependent interdiffusion coefficients requires the use of the Boltzmann-Matano analysis with two independent diffusion couples that develop a common composition in the diffusion zone. Instead, the interdiffusion fluxes $\tilde{J}_i$ of all components can be determined directly from their concentration profiles of an infinite diffusion couple without the need of the interdiffusion coefficients on the basis of the relation:[31]

$$\tilde{J}_i = \frac{1}{2t} \int_{C_i^- \text{or} C_i^+}^{C_i(\text{x})} (x - x_\text{o}) dC_i \quad (i = 1, 2, \ldots, n) \qquad \text{(Eq 2)}$$

where t is the time, C_i^- and C_i^+ are the terminal concentrations of the alloys used for the couple, and x_o refers to the location of the Matano plane.

The interdiffusion flux $\tilde{J}_i$, determined from Eq 2 can be integrated with respect to position x to define the average effective interdiffusion coefficient $\tilde{D}_i^{\text{eff}}$:[32]

$$\tilde{D}_i^{\text{eff}} = \frac{\int_{\text{x}_1}^{\text{x}_2} \tilde{J}_i dx}{C_i^{x_2} - C_i^{x_1}} \quad (i = 1, 2, 3) \qquad \text{(Eq 3)}$$

This effective interdiffusion coefficient incorporates all multicomponent diffusional interactions for the system to provide an effective value for the interdiffusion of a component species as defined by:

$$\tilde{D}_i^{\text{eff}} = \tilde{D}_{ii}^n + \sum_j \frac{\tilde{D}_{ij}^n \partial C_j/\partial x}{\partial C_i/\partial x} \quad (i \neq j) \qquad \text{(Eq 4)}$$

The interdiffusion flux $\tilde{J}_i$, determined from Eq 2 as a function of x, can be multiplied by $(x - x_o)^n$ and integrated over a selected region, x_1 to x_2; in the light of Eq 1, one gets:[33]

$$\int_{x_1}^{x_2} \tilde{J}_i (x - x_\text{o})^n \, dx = -\bar{\tilde{D}}_{i1}^3 \int_{C_1(x_1)}^{C_1(x_2)} (x - x_\text{o})^n dC_1 - \bar{\tilde{D}}_{i2}^3 \int_{C_2(x_1)}^{C_2(x_2)} (x - x_\text{o})^n dC_2 \quad (i, j = 1, 2) \qquad \text{(Eq 5)}$$

where $\bar{\tilde{D}}_{ij}^3$ (i, j = 1,2) coefficients are the average values of main and cross-interdiffusion coefficients treated as constants over the selected composition range. Equation 5 can provide four equations involving the $\bar{\tilde{D}}_{ij}^3$ interdiffusion coefficients (n = 0, 1, or 2) and can be set up from interdiffusion fluxes calculated on the basis of Eq 2 from the concentration profiles of a single diffusion couple. The $\bar{\tilde{D}}_{ij}^3$ coefficients, characteristic of the diffusion path, can be determined over selected composition ranges that include the nonlinear segment of the profiles.[33] The determination of ternary interdiffusion coefficients by using Eq 5 does not require the use of concentration gradients (i.e., $\partial C_i/\partial x$), and significantly reduces the uncertainty involved in the determination of interdiffusion coefficients arising from microprobe measurement and the concentration smoothening procedure.[33]

Table 1 Compositions of Ni-Cr-X alloys employed for solid-to-solid diffusion couples

Alloy identification	Composition, atom fraction			Composition, weight fraction		
	Ni	Cr	X	Ni	Cr	X
Ni	100.0	…	…	100	…	…
NiCr (X = None)	78.0	22.0	…	80	20	…
NiCrAl (X = Al)	72.5	21.3	6.2	77	20	3
NiCrSi (X = Si)	74.0	22.0	4.0	78	20	2
NiCrGe (X = Ge)	76.3	22.1	1.6	78	20	2
NiCrPd (X = Pd)	76.1	22.3	1.6	77	20	3

3. Experimental Procedure

Binary and ternary alloys with compositions reported in Table 1 were prepared with 99.9% pure Ni, Cr, Al, Si, Ge, and Pd by arc melting under an argon (Ar) atmosphere. The alloys were chill-cast by water-cooled copper mold into

Table 2 List of Ni versus Ni-Cr-X and NiCr versus Ni-Cr-X solid-to-solid diffusion couples annealed at 900 °C for 168 h

Series	Diffusion couples
I	Ni vs. Ni-Cr
II	Ni vs. Ni-Cr-Al
	Ni vs. Ni-Cr-Si
	Ni vs. Ni-Cr-Ge
	Ni vs. Ni-Cr-Pd
III	Ni-Cr vs. Ni-Cr-Al
	Ni-Cr vs. Ni-Cr-Si
	Ni-Cr vs. Ni-Cr-Ge
	Ni-Cr vs. Ni-Cr-Pd

rods with a vacuum ~12 mm in diameter. The alloy rods were placed in a quartz tube, evacuated to a pressure $<10^{-6}$ torr, and flushed with hydrogen. This hydrogen-flushing procedure was repeated several times, and a quartz capsule was filled with Ar before the final seal. They were homogenized at 900 °C for 168 h in a horizontal Lindberg three-zone tube furnace and water-quenched to preserve the high-temperature microstructure. The microstructures and compositions of the alloys were examined by optical microscopy, scanning electron microscopy, energy dispersive spectroscopy, and electron microprobe analysis (EPMA). No measurable variation in the alloy compositions was observed, and all alloys consisted of face-centered cubic (fcc) Ni solid solution (γ phase).

Diffusion disks with approximate thicknesses of 2 mm were cut from the rods of alloys and were prepared metallographically by polishing with 0.25 μm diamond paste. Table 2 presented ternary diffusion couples that were assembled with the disks held together in an Invar steel jig consisting of two end plates and three threaded rods. The couples were placed in quartz capsules, which were sealed at one end, evacuated to a pressure $<10^{-6}$ torr, and flushed with hydrogen several times. A capsule was filled with Ar before the final sealing. The capsules containing the couples were annealed at 900 °C in a horizontal Lindberg three-zone furnace for 168 h. After the anneal, the couples were quenched in water to preserve the high-temperature microstructures.

The diffusion assembly was then mounted, sectioned, and metallographically prepared for microstructural observations. Excellent bonding within all diffusion couples was observed. Then, the cross section surface was repolished with 1 μm diamond paste for EPMA. The concentration profiles of Ni, Cr, Al, Si, Ge, and Pd for the diffusion couples were determined with a JEOL 733 (Tokyo, Japan) microprobe by point-to-point counting techniques using pure Ni, Cr, Al, Si, Ge, and Pd as standards. Intensities of K_α *X*-radiation were measured and converted to concentrations of Ni, Cr, Al, Si, Ge, and L_α *X*-radiation for that of Pd with appropriate ZAF (atomic number, Z; absorption, A; fluorescence, F) corrections. Concentration profiles obtained from EPMA was smoothened by a weighted spline tool using MatLab (The Math Works, Natick, MA). It should be noted that the analytical method used in this study to determine interdiffusion coefficients by the integration of interdiffusion fluxes (e.g., Eq 5) do not require the use of concentration gradients. This method significantly reduces the influence of a smoothening procedure on the determination of interdiffusion coefficients.

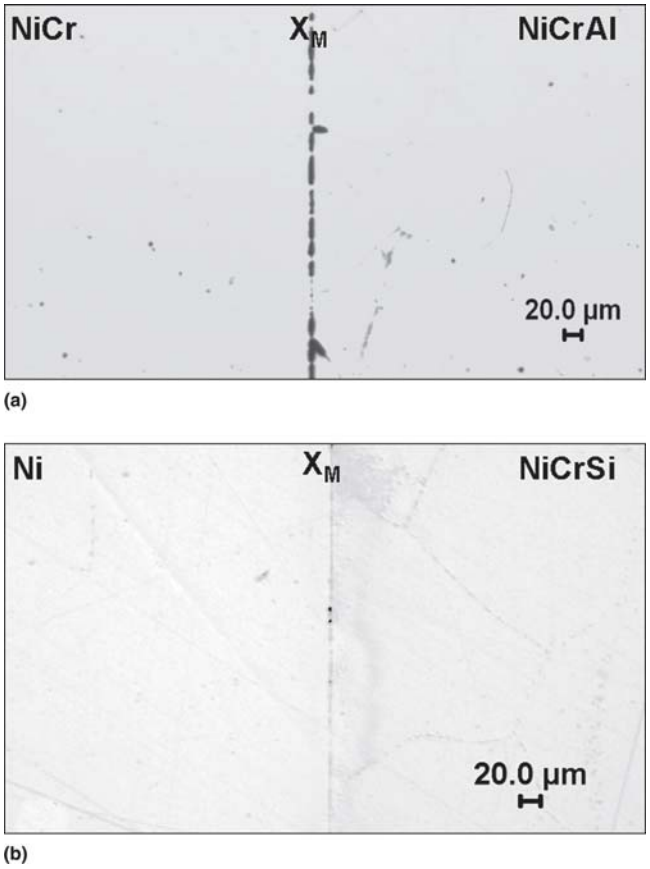

Fig. 1 Typical optical micrographs of solid-to-solid diffusion couples etched with Kallings reagent: (a) Ni-Cr versus Ni-Cr-Al and (b) Ni versus Ni-Cr-Si annealed at 900 °C for 168 h. Specimens were slightly overetched to clearly distinguish the experimental contact plane x_m.

4. Results and Discussion

Figure 1 presents an optical micrograph obtained from the diffusion couples Ni versus Ni-Cr-Al and Ni versus Ni-Cr-Si that was annealed at 900 °C for 168 h. Excellent bonding was achieved during the diffusion anneal for all diffusion couples. Figure 2 presents an example of the experimental and smoothened concentration profiles that were used for the determination of interdiffusion coefficients. The scatters in the concentration profiles for all diffusion couples were minimal and within the experimental uncertainty associated with EPMA. Experimental concentration profiles were smoothened with a weighted-spline routine by using MatLab.

From concentration profiles obtained from series I and II diffusion couples (i.e., Ni versus Ni-Cr, and Ni versus

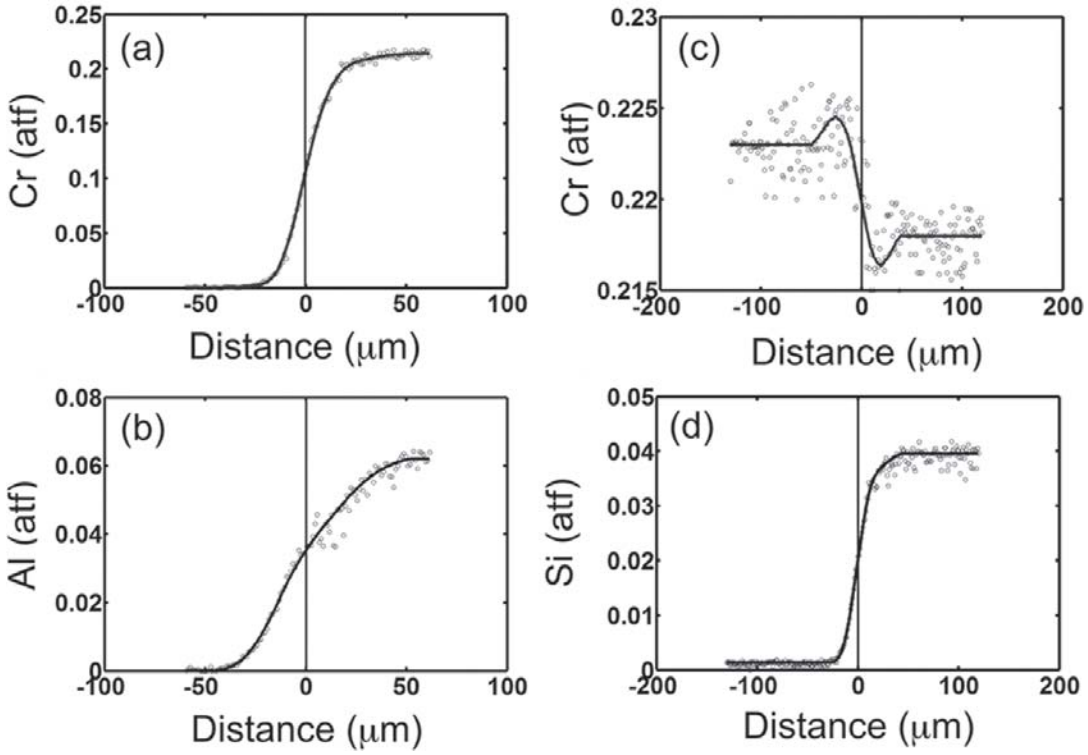

Fig. 2 Typical experimental and smoothened concentration profiles measured from solid-to-solid diffusion couples (a, b) Ni vs. Ni-Cr-Al and (c, d) Ni-Cr vs. Ni-Cr-Si, annealed at 900 °C for 168 h

Ni-Cr-*X*, respectively), the average effective interdiffusion coefficients $\tilde{D}_i^{\text{eff}}$ on either side of the Matano plane were determined using Eq 3. In general, $\tilde{D}_i^{\text{eff}}$ was higher on the $(C_i^{\text{o}} \sim C_i^{+\infty})$ composition range with a higher Cr concentration relative to the other side of the Matano plane. Table 3 also reports that an Al addition to a NiCr alloy can increase or decrease the $\tilde{D}_{\text{Cr}}^{\text{eff}}$ as a function of composition. This indicates appreciable variation in interdiffusion coefficients as a function of composition: specifically, Al increased $\tilde{D}_{\text{Cr}}^{\text{eff}}$ on the $(C_i^{\text{o}} \sim C_i^{+\infty})$ composition range with a higher Cr concentration. $\tilde{D}_{\text{Cr}}^{\text{eff}}$ was observed to increase with an Si addition to a NiCr alloy, especially on the $(C_i^{\text{o}} \sim C_i^{+\infty})$ side with higher Cr concentration. According to Table 3, Ge does not change $\tilde{D}_{\text{Cr}}^{\text{eff}}$ significantly, while a Pd addition to an Ni-Cr alloy increased $\tilde{D}_{\text{Cr}}^{\text{eff}}$, which is quite significant on the $(C_i^{\text{o}} \sim C_i^{+\infty})$ range with a higher Cr concentration.

From concentration profiles obtained from diffusion couple series I and II (i.e., Ni versus Ni-Cr, and Ni versus Ni-Cr-*X*, respectively), average ternary interdiffusion coefficients $\tilde{\bar{D}}_{ij}^{\text{Ni}}(i,j = \text{Cr}, X)$ were determined on either side of the Matano plane using Eq 5. These diffusion couples are reported in Table 4. It should be noted that these diffusion couples were designed to yield the same sign of $\partial C_{\text{Cr}}/\partial x$ and $\partial C_X/\partial x$. Thus, positive and negative $\tilde{\bar{D}}_{\text{Cr}X}^{\text{Ni}}$ indicates an increase and a decrease in $\tilde{J}_{\text{Cr}}$, respectively. In general, larger magnitudes of $\tilde{\bar{D}}_{\text{CrCr}}^{\text{Ni}}$ and $\tilde{\bar{D}}_{XX}^{\text{Ni}}$ were observed on the $(C_i^{\text{o}} \sim C_i^{+\infty})$ composition range with higher Cr concentration. The Al addition in the Ni-Cr alloy yielded positive $\tilde{\bar{D}}_{\text{CrAl}}^{\text{Ni}}$, and increased $\tilde{J}_{\text{Cr}}$ in accordance with previous work by Nesbitt and Heckel[25] and Thompson et al.[34] The magnitude of $\tilde{\bar{D}}_{\text{CrAl}}^{\text{Ni}}$ was quite large, as reported in Table 4 on the $(C_i^{\text{o}} \sim C_i^{+\infty})$ with higher Cr concentration. Similarly, Si, Ge, and Pd additions to the Ni-Cr alloy increased $\tilde{J}_{\text{Cr}}$ with positive $\tilde{\bar{D}}_{\text{Cr}X}^{\text{Ni}}$. This effect was, again, stronger when the Cr concentration was high on the $(C_i^{\text{o}} \sim C_i^{+\infty})$, particularly for Si and Pd.

Table 3 Average effective interdiffusion coefficients determined from Ni vs. Ni-Cr-X diffusion couples annealed at 900 °C for 168 h

Diffusion couple	Composition range	$\tilde{D}_{\text{Cr}}^{\text{eff}}$, 10^{-16} m^2/s	$\tilde{D}_x^{\text{eff}}$, 10^{-16} m^2/s	$\tilde{D}_{\text{Ni}}^{\text{eff}}$, 10^{-16} m^2/s
Ni vs. Ni-Cr	$(C_i^{-\infty} \sim C_i^{\text{o}})$	1.40	…	1.40
(X = None)	$(C_i^{\text{o}} \sim C_i^{+\infty})$	1.53	…	1.53
Ni vs. Ni-Cr-Al	$(C_i^{-\infty} \sim C_i^{\text{o}})$	0.91	3.31	1.83
(X = Al)	$(C_i^{\text{o}} \sim C_i^{+\infty})$	1.58	4.68	2.19
Ni vs. Ni-Cr-Si	$(C_i^{-\infty} \sim C_i^{\text{o}})$	1.68	5.74	2.26
(X = Si)	$(C_i^{\text{o}} \sim C_i^{+\infty})$	3.00	6.91	3.57
Ni vs. Ni-Cr-Ge	$(C_i^{-\infty} \sim C_i^{\text{o}})$	1.30	3.09	1.40
(X = Ge)	$(C_i^{\text{o}} \sim C_i^{+\infty})$	1.44	3.47	1.61
Ni vs. Ni-Cr-Pd	$(C_i^{-\infty} \sim C_i^{\text{o}})$	1.77	1.19	1.74
(X = Pd)	$(C_i^{\text{o}} \sim C_i^{+\infty})$	4.09	2.07	3.92

Diffusion couple series III was designed with initial $\partial C_{\text{Cr}}/\partial x = 0$, so that $\tilde{J}_{\text{Cr}}$ is largely due to $\partial C_X/\partial x$, and depends on the magnitude and sign of $\tilde{\bar{D}}_{\text{Cr}X}^{\text{Ni}}$. $\tilde{J}_X$ has caused an uphill diffusion of Cr in the direction of J_X with positive $\tilde{\bar{D}}_{\text{Cr}X}^{\text{Ni}}$ for Al and Si. This indicates that Al and Si should increase the thermodynamic activity of Cr in Ni-Cr alloys.

Table 4 Average ternary interdiffusion coefficients determined from Ni vs. Ni-Cr-X diffusion couples annealed at 900 °C for 168 h

Diffusion couple	Composition range	$\tilde{\tilde{D}}^{Ni}_{CrCr}$, 10^{-16} m^2/s	$\tilde{\tilde{D}}^{Ni}_{CrX}$, 10^{-16} m^2/s	$\tilde{\tilde{D}}^{Ni}_{XCr}$, 10^{-16} m^2/s	$\tilde{\tilde{D}}^{Ni}_{XX}$, 10^{-16} m^2/s
Ni vs. Ni-Cr-Al (X = Al)	$(C_i^{-\infty} \sim C_i^o)$	0.78	0.31	0.40	1.99
	$(C_i^o \sim C_i^{+\infty})$	1.11	1.72	0.43	2.84
Ni vs. Ni-Cr-Si (X = Si)	$(C_i^{-\infty} \sim C_i^o)$	1.23	0.15	0.44	2.92
	$(C_i^o \sim C_i^{+\infty})$	2.05	4.88	0.57	3.35
Ni vs. Ni-Cr-Ge (X = Ge)	$(C_i^{-\infty} \sim C_i^o)$	1.08	0.36	0.07	1.73
	$(C_i^o \sim C_i^{+\infty})$	1.24	0.89	0.10	1.99
Ni vs. Ni-Cr-Pd (X = Pd)	$(C_i^{-\infty} \sim C_i^o)$	1.43	4.06	0.01	0.98
	$(C_i^o \sim C_i^{+\infty})$	3.49	4.86	0.01	1.76

Table 5 Average ternary interdiffusion coefficients determined from Ni-Cr vs. Ni-Cr-X diffusion couples annealed at 900 °C for 168 h

Diffusion couple	Composition range	$\tilde{\tilde{D}}^{Ni}_{CrCr}$, 10^{-16} m^2/s	$\tilde{\tilde{D}}^{Ni}_{CrX}$, 10^{-16} m^2/s	$\tilde{\tilde{D}}^{Ni}_{XCr}$, 10^{-16} m^2/s	$\tilde{\tilde{D}}^{Ni}_{XX}$, 10^{-16} m^2/s
Ni-Cr vs. Ni-Cr-Al (X = Al)	$(C_i^{-\infty} \sim C_i^o)$	0.23	0.12	0.01	0.67
	$(C_i^o \sim C_i^{+\infty})$	1.20	0.44	0.13	1.17
Ni-Cr vs. Ni-Cr-Si (X = Si)	$(C_i^{-\infty} \sim C_i^o)$	2.58	1.73	0.01	0.68
	$(C_i^o \sim C_i^{+\infty})$	1.39	0.63	1.78	1.97
Ni-Cr vs. Ni-Cr-Ge (X = Ge)	$(C_i^{-\infty} \sim C_i^o)$				
	$(C_i^o \sim C_i^{+\infty})$				
Ni-Cr vs. Ni-Cr-Pd (X = Pd)	$(C_i^{-\infty} \sim C_i^o)$				

$\Delta C_{Cr}/\Delta x = 0$ and cannot be determined.

On the other hand, $\tilde{J}_{Ge}$ and $\tilde{J}_{Pd}$ did not cause any measurable redistribution of Cr ($\tilde{J}_{Cr} \approx 0$). It should be noted that Ge and Pd have lower contents in the Ni-Cr-X alloys than Al and Si, as reported in Table 1.

Based on the average effective interdiffusion coefficients and average ternary interdiffusion coefficients determined in this study, alloying additions of Al, Si, Ge, and Pd have all increased $\tilde{D}^{eff}_{Cr}$ and yielded positive $\tilde{\tilde{D}}^{Ni}_{CrX}$ particularly with high Cr content (~22 at.%). Therefore, the Cr_2O_3-forming ability of the Ni-20at.%Cr-based alloy should improve with these alloying additions by establishing Cr_2O_3 scale, by maintaining protective Cr_2O_3 scale formation, and in reformation of Cr_2O_3 on spallation. It should be noted that the positive $\tilde{\tilde{D}}^{Ni}_{XCr}$ reported in Tables 4 and 5 should also promote the formation of other scales (Al_2O_3, SiO_2) in the γ (fcc) Ni-Cr alloy, which may reduce the rate of scale growth and/or change the thermomechanical properties of the scale.

5. Summary

Based on experimental solid-to-solid diffusion couples, a small addition of Al, Si, Ge, or Pd was observed to increase the overall interdiffusion flux of Cr in Ni-22at.%Cr-X (fcc γ phase) alloys. Experimental concentration profiles, measured after annealing at 900 °C in a three-zone tube furnace for 168 h, were used to determine interdiffusion fluxes, average effective interdiffusion coefficients, and average ternary interdiffusion coefficients. In general, $\tilde{D}^{eff}_i$ was observed to increase with a higher Cr concentration. Also, $\tilde{\tilde{D}}^{Ni}_{CrX}$ coefficients were determined to be positive with alloying additions of Al, Si, Ge, or Pd. These results suggest that these alloying additions can help the formation of Cr_2O_3 scale for initial scale formation, maintaining scale homogeneity during prolonged high-temperature exposure, and for reformation after scale spallation.

Acknowledgments

This work was supported by the National Science Foundation CAREER Award under the grant DMR-0238356 (Y.H. Sohn) and U.S. Department of Energy, Fossil Energy Advanced Research Materials (ARM) program. Oak Ridge National Laboratory is managed by UT-Battelle, LLC, for the U.S. Department of Energy under contract DE-AC05-00OR22725.

References

1. C.T. Sims, N.S. Stoloff, and W.C. Hagel, *Superalloys II,* John Wiley and Sons, 1987
2. P. Kofsted, Growth and Protective Properties of Chromia (Cr_2O_3) and Alumina (Al_2O_3) Scales, Protective Coatings, *High Temperature Corrosion,* Elsevier, London, 1980, p 389-423
3. J.L. Smialek, C.A. Barrett, and J.C. Schaffer, Design for Oxidation Resistance, *ASM Handbook, Vol. 20, Materials Selection and Design,* George E. Dieter, Ed., ASM International, 1997, p 589-602
4. F.H. Stott, G.C. Wood, and M.G. Hobby, A Comparison of the

Oxidation Behavior of Fe-Cr-Al, NI-Cr-Al and Co-Cr-Al Alloys, *Oxid. Met.,* 1971, **3,** p 103-113
5. C.E. Lowell, A Scanning Electron Microscope Study of the Surface Morphology of TD-NiCr Oxidized at 800 °C to 1200 °C, *Oxid. Met.,* 1972, **5,** p 205-220
6. C.E. Lowell, Cyclic and Isothermal Oxidation Behavior on Some Ni-Cr Alloys, *Oxid. Met.,* 1973, **7,** p 95-115
7. G.M. Ecer and G.H. Meier, Oxidation of High-Ehromium Ni-Cr Alloys, *Oxid. Met.,* 1979, **13,** p 119-158
8. G. Benabderrazik, G. Moulin, and A.M. Huntz, Relation Between Impurities and Oxide-Scale Growth Mechanisms on Ni-34Cr and Ni-20Cr Alloys: I. Influence of C, Mn, and Si, *Oxid. Met.,* 1990, **33,** p 191-235
9. J.F. Schmitt, N. Pacia, P. Pigeat, and B. Weber, Study of the Initial Oxidation of a Ni-20Cr Alloy in the Temperature Range 550–830 °C: Influence of Mechanical Deformation, *Oxid. Met.,* 1995, **44,** p 429-452
10. C.K. Kim and L.W. Hobbs, Microstructural Evidence for Short-Circuit Oxygen Diffusion Paths in the Oxidation of a Dilute Ni-Cr Alloy, *Oxid. Met.,* 1996, **45,** p 247-265
11. B. Ahmad and P. Fox, STEM Analysis of the Transient Oxidation of a Ni-20Cr Alloy at High Temperature, *Oxid. Met.,* 1998, **52,** p 113-138
12. J.R. Nicholls and M.J. Bennett, Cyclic Oxidation-Guidelines for Test Standardization, Aimed at the Assessment of Service Behavior, *Mater. High Temp.,* 2000, **17,** p 413-428
13. B. Li and B. Gleeson, Effect of Silicon on Oxidation Behavior of Ni-Base Chromia-Forming Alloys, *Oxid. Met.,* 2006, **65,** p 101-122
14. F.H. Stott, G.C. Wood, and J. Stringer, The Influence of Alloying Elements on the Development and Maintenance of Protective Scales, *Oxid. Met.,* 1995, **44,** p 113-145
15. D.P. Whittle and J. Stringer, Improvements in High Temperature Oxidation Resistance by Additions of Reactive Elements or Oxide Dispersions, *Proc. R. Soc. Lond., Ser. A,* 1980, **295,** p 309-329
16. G.C. Wood and F.H. Scott, Oxidation of Metals, *Mater. Sci. Technol.,* 1987, **3,** p 519-530
17. G.C. Wood, J.A. Richards, M.G. Hobby, and J. Boustead, Identification of Thin Healing Layers at Based of Oxide Scale on Fe-Cr Base Alloys, *Corros. Sci.,* 1969, **9,** p 659-671
18. A.G. Revsz and F.P. Fehlner, The Role of Noncrystalline Films in the Oxidation and Corrosion of Metals, *Oxid. Met.,* 1981, **15,** p 297-321
19. M.J. Bennett, J.A. Desport, and P.A. Labun, Analytical Electron Microscopy of a Selective Oxide Scale Formed on 20% Cr-25% Ni-Nb Stainless Steel, *Oxid. Met.,* 1984, **22,** p 291-306
20. M.J. Bennett, J.A. Despota, and P.A. Labun, Transverse Microstructue of an Oxide Scale Formed on a 20%Cr-25%Ni-Nb Stabilized Stainless Steel, *Proc. R. Soc. Lond., Ser. A,* 1987, **412**, p 223-230
21. R.C. Lobb, J.A. Sasse, and H.E. Evans, Dependence of Oxidation Behavior on Silicon Content of 20%Cr Austenitic Steels, *Mater. Sci. Technol.,* 1989, **5,** p 828-834
22. W.C. Hagel, Oxidation of Iron Nickel and Cobalt-Base Alloys Containing Aluminum, *Corrosion,* 1965, **21,** p 316-326
23. J.A. Nesbitt, Numerical Modeling of High-Temperature Corrosion Processes, *Oxid. Met.,* 1995, **44,** p 309-338
24. H.E. Evans, A.T. Donaldson, and T.C. Gilmour, Mechanisms of Breakaway Oxidation and Application to a Chromia-Forming Steel, *Oxid. Met.,* 1999, **52,** p 379-402
25. J.A. Nesbitt and R.W. Heckel, Interdiffusion in Ni-Rich, Ni-Cr-Al Alloys at 1100 and 1200 °C: Part I. Diffusion Paths and Microstructures, *Metall. Trans. A,* 1987, **18A,** p 2061-2086
26. C.S. Giggin and F.S. Pettit, Oxidation of Ni-Cr-Al Alloys Between 1000 and 1200 °C, *J. Electrochem. Soc.,* 1971, **118,** p 1782-1790
27. B.A. Pint, J.R. Keiser, "Alloy Selection for High Temperature Heat Exchangers," NACE Paper 06-469, presented at NACE Corrosion 2006 (San Diego, CA), NACE International, March 2006
28. M.P. Brady, B. Gleeson, and I.G. Wright, Alloy Design Strategies for Promoting Protective Oxide Scale Formation, *JOM,* 2000, **52,** p 16-21
29. D.J. Young and B. Gleeson, Alloy Phase Transformations Driven by High Temperature Corrosion Processes, *Corros. Sci.,* 2002, **44,** p 345-357
30. L. Onsager, Theories and Problems of Liquid Diffusion, *Ann. N. Y. Acad. Sci.,* 1965, **46,** p 241-265
31. M.A. Dayananda and C.W. Kim, Zero-Flux Planes and Flux Reversals in Cu-Ni-Zn Diffusion Couples, *Metall. Trans. A,* 1979, **10A,** p 1333-1339
32. M.A. Dayananda and Y.H. Sohn, Average Effective Interdiffusion Coefficients and Their Applications for Isothermal Multicomponent Diffusion Couples, *Scr. Mater.,* 1996, **40,** p 683-688
33. M.A. Dayananda and Y.H. Sohn, A New Approach for the Determination of Interdiffusion Coefficients in Ternary Systems, *Metall. Mater. Trans. A,* 1999, **30A,** p 535-543
34. M.S. Thompson, J.E. Morral, and A.D. Romig Jr., Applications of the Square Root Diffusivity to Diffusion in Ni-Al-Cr Alloys, *Metall. Trans. A,* 1990, **21A,** p 2679-2685